CHALMERS
UNIVERSITY OF TECHNOLOGY

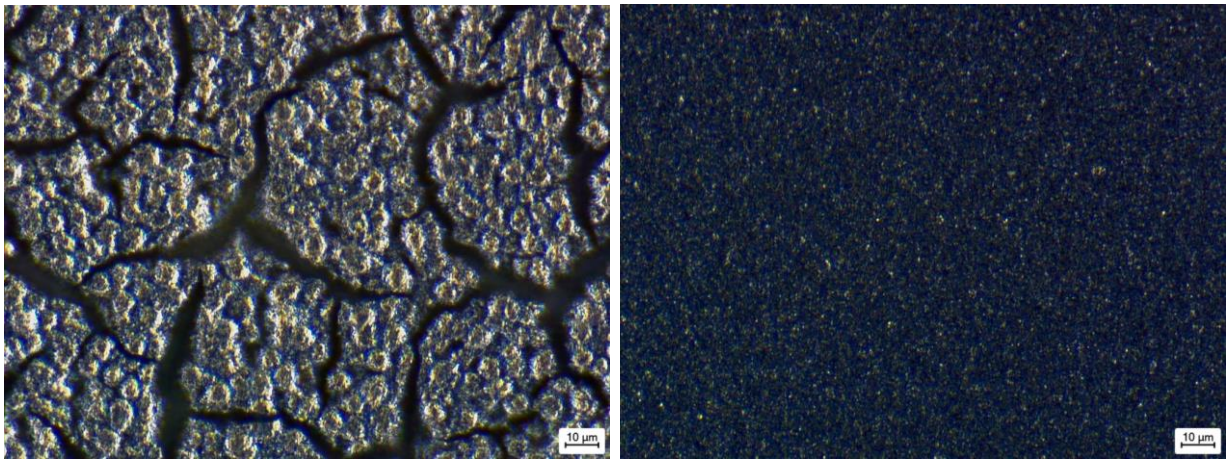

Investigation of the influence of coating and drying methods of catalytic inks on the structure of resulting electrodes for Proton Exchange Membrane Fuel Cells

Master's thesis in Physics

SANDEEP JAYAPRAKASH NAIR

DEPARTMENT OF PHYSICS

CHALMERS UNIVERSITY OF TECHNOLOGY

Gothenburg, Sweden 2023
www.chalmers.se

MASTER'S THESIS 2023

Investigation of the influence of coating and drying methods of catalytic inks on the structure of resulting electrodes for Proton Exchange Membrane Fuel Cells

SANDEEP JAYAPRAKASH NAIR

Supervisor: Felix Ernst, PowerCell Group
Examiner: Björn Wickman, Department of Physics

CHALMERS
UNIVERSITY OF TECHNOLOGY

Cover: Microscope pictures of catalyst electrode coatings showing cracked electrodes on the left and crack free electrodes on the right.

DEPARTMENT OF PHYSICS
CHALMERS UNIVERSITY OF TECHNOLOGY
Gothenburg, Sweden 2023
www.chalmers.se

Investigation of the influence of coating and drying methods of catalytic inks on the structure of resulting electrodes for Proton Exchange Membrane Fuel Cells

SANDEEP JAYAPRAKASH NAIR
Department of Physics
Chalmers University of Technology

Abstract

In the decal transfer process of making catalyst electrode coatings for Proton Exchange Membrane Fuel Cells (PEMFCs), understanding the coating and drying parts of the process is important to get desired final electrode structures. Coating and drying are also important manufacturing steps and must be optimized for this as well. The structural evolution during drying from ink microstructure to the electrode microstructure yields the resulting pore structure at a micro scale, and at a larger length scale the crack morphology. To achieve the desired structures, we need to make both a well dispersed catalyst ink with good interaction of components and provide favorable drying conditions.

In this study, different solvent combinations and dry weights in ink, and different drying conditions of temperature and vapor pressures were explored. Qualitative inspection of digital microscope images of the electrodes was used to analyze dried structure and cracks. Critical Crack Thickness (CCT), the height up to which a coating can inhibit cracks well, and the maximum catalyst loading in each setting was monitored. Results showed that 1-propanol rich solvent matrix with water gave the least cracks and highest CCTs in comparison to ethanol and tert-butanol for the studied catalyst and ionomer. Higher temperatures did not have a strong impact on crack morphology or CCT for the same ink recipes but reduced the drying time. Higher vapor pressure of alcohol above the wet ink coating led to slower drying and enabled higher CCTs. The experiments enabled us to achieve coatings with a loading of 0.7 mg/cm^2 and a CCT of 250 microns, robust to higher temperature drying conditions, which was not possible before with recipes described by suppliers. The results here are promising for making high performance electrodes in-house and has set a foundation for future work on fuel cells for a variety of applications, helping the green energy transition.

Keywords: fuel cells, catalyst ink, catalyst electrode, coating and drying, ionomer, solvent matrix, catalyst loading, CCT, decal transfer, microstructure, rheology, microscopy

Acknowledgements

I am grateful for the guidance of my supervisor Felix Ernst, and my examiner Björn Wickman. Special thanks to the support from Gabor Toth, Parinaz Mikaeli, and Marika Männikkö at PowerCell. Thanks to my wonderful colleagues Nora Malmquist, Emma Ulberstad, and Dylan Schulz. To all my friends at Chalmers, this wouldn't have been possible without our infamous work sessions. Finally, I would like to thank my family for their love and support throughout my thesis journey.

SANDEEP,
Gothenburg, 2023

List of Acronyms

FC – Fuel Cell
PEMFC – Proton Exchange Membrane Fuel Cell
MEA – Membrane Electrode Assembly
SEM – Scanning Electron Microscope
Pt/C – Platinum on Carbon
CCT – Critical Crack Thickness
NPA – N-propyl Alcohol
IPA – Iso-propyl Alcohol
ET – Ethanol
TB – Tert-butanol
EG – Ethylene Glycol
BUT – Butane Diol
USAXS – Ultra-Small Angle X-ray Scattering
DLS – Dynamic Light Scattering
PFSA – Poly Fluro Sulphonic Acid
HDPE – High Density Polyethylene
MA – Moisture Analyzer
CCM – Catalyst Coated Membrane
PTFE – Poly Tetra Fluro Ethylene
I/C – Ionomer is to Catalyst
HNxy – Water:NPA, x – number in ratio for water, y – number in ratio for NPA
HExy – Water:ET, x – number in ratio for water, y – number in ratio for ET
HTxy – Water:TB, x – number in ratio for water, y – number in ratio for TB
VP – Vapor Pressure

Contents

List of Figures

List of Tables

1. Introduction

1.1. Background

With the global energy demand on the rise, producing energy in ways that do not harm the environment adversely is important for the future. A lot of today's energy demands worldwide are met by burning fossil fuels. Fossil fuels have limited reserves. Combustion of such fuels for energy emits carbon dioxide which increases global warming and creates other toxic by-products. This calls for technologies that use sustainable energy sources and do not produce harmful emissions. The fuel cell (FC) is an energy conversion technology that meets these requirements.

A fuel cell is an electrochemical device that converts the chemical energy of a fuel into electricity. There are different types of fuel cells based on the electrolyte materials and fuels used. Proton exchange membrane fuel cell (PEMFC), solid oxide fuel cell (SOFC), direct methanol fuel cell (DMFC), alkaline fuel cell (AFC), and molten carbonate fuel cell (MCFC) are some examples. Of these, the PEMFC is currently the most researched, advanced, and commercialized fuel cell technology [1]. It uses hydrogen as fuel and converts it to electricity, producing only water and heat as by-products. It has advantages over other fuel cell technologies like higher energy density, faster start-up time, and better performance at low temperatures. Energy density in fuel cells can also be higher in comparison to other clean conversion technologies like batteries. This has advantages in several applications, like off-road tractors and trucks, which benefit from a longer driving range.

A PEMFC works by passing reactant gases (hydrogen and oxygen) onto electrodes separated by a polymer electrolyte membrane (PEM). The electrode where the oxygen reduction reaction (ORR) takes place is the cathode, and the electrode where the hydrogen oxidation reaction (HOR) takes place is the anode. The PEM selectively passes the protons generated in the reaction at the anode onto the cathode, and the electrons are passed through an external circuit, where it is used as output electricity, before reaching the cathode. The electrodes are porous, thin layers, made up of three key components: the precious metal catalyst, the carbon support structure, and the ionomer. The precious metal catalyst promotes the reactions at the electrodes, and the carbon support provides electron conduction pathways. The ionomer is a functionalized polymer, made of similar materials as the PEM. It functions as the proton conducting material as well as a binder that holds the layer together. The interactions of the three components can be complex and decide the final electrode structure. For the best performance, the electrodes need to simultaneously support processes like high reactant transport, catalytic activity, charge transport, and water removal [2]. This can be achieved by designing and optimizing the structure of the electrodes through the manufacturing process used.

There are different ways to make an electrode layer. Most current techniques involve making a catalyst ink first, in which all the components of the electrode are dispersed in a

solvent mixture. This ink is then coated on a polymer substrate and dried. It can then be transferred onto the PEM using a specialised press machine. The polymer substrate on which the coating is made is referred to as the decal and this method is called the decal transfer method. This is a reliable method and can be scaled up easily for production. The drying of the catalyst ink on the decal is a key step. The structural evolution of the catalyst ink during drying decides the final electrode microstructure and morphology. Developments in the drying process can enable better performance and durability, which are the main targets of an improved fuel cell product. It is therefore a big area of interest for research in the electrode manufacturing process.

1.2. Research Question

My thesis is taking a deeper look into the ink coating and drying steps in the process of electrode development. The objective is to understand how the different parameters mainly in these steps of the process affect the structure of the dried coating, and to improve electrode quality by reducing the occurrence of defects like cracks and agglomerates. I have also tried to make such electrodes of improved quality at higher catalyst loadings (amount of catalyst present per unit area in an electrode).

The parameters considered can be divided into three blocks: catalyst ink composition parameters, coating process parameters, and drying process parameters. In catalyst ink composition, the solid content of the ink, the ionomer to catalyst ratio, and the solvent combinations used, were the parameters considered. In the coating process, the gap height of the blade coater and the speed of coating were the parameters considered. And in the drying process, the drying temperature and the vapor pressure of solvent above the coating were the parameters considered. Impact of using different decal substrate materials were also considered after measurement of their surface properties. The results of the experiments were evaluated mainly with a qualitative analysis of microscope pictures and catalyst loading measurements of the dried electrode coatings.

1.3. Hypothesis

There is an optimum catalyst ink composition that leads to a better structure in the dried coating. Both increasing and decreasing the solid content and ionomer to catalyst ratio from this optimum will lead to worse results. Changing the solvent combination used will influence the ink structure and lead to very different structures in the dried coatings. Higher gap heights of the blade coater will lead to thicker coatings with a higher catalyst loading. Higher gap height of the blade coater will also lead to drying stresses and therefore more cracks. Higher temperatures while drying will lead to faster drying, which leads to higher drying stresses and therefore more cracks. Higher vapor pressures of the solvent above the coatings will lead to a slower and more uniform drying process, reducing the drying stresses

and cracks in the coatings. Different decal substrate materials with similar surface properties should lead to similar structures in the dried coatings.

1.4. Limitations

Optimizing the process from ink making to getting the final dried coatings is a huge multi-parameter problem. For limiting the scope of this thesis only some parameters of interest are considered. This may lead to a different optimum point than if all parameters were considered. It is assumed that the knowledge gained here will still be useful for competence build-up in the process development of electrode making. Dispersion energy and power input into the ink are not investigated. A constant high value of energy is used throughout, and it is assumed that this is a good enough dispersion process for all the ink trials. Ink behaviour is very time dependant. But this is too tedious to closely monitor during the thesis. Ink maturation time is kept constant throughout, and other time evolution related effects are not considered. Characterization techniques to study ink microstructure (does not let light pass through, making light-based characterisations difficult) and the dried electrode structure (the ionomer is a polymer with no crystal structure and can be as small as a few nanometres thick around the Pt/C agglomerates making it very difficult to map) are limited and challenging to perform. The drying process of catalyst ink and the structural evolution during drying is a complex process. Academic literature and existing knowledge on the topic are limited.

2. Theory

2.1. Drying of thin coatings

A general outline of the drying process applicable to most thin coatings is a good starting point to build on for further studies. Drying of a thin coating of solids dispersed in solvent medium proceeds in stages. Four such stages are the initial liquid stage, the gelation stage, the capillary formation stage, and the final solidification stage [4]. Starting from the liquid stage, as solvent evaporates, the solid particles come closer together till they reach close enough to start gelling. The solid particles will move less relative to each other after this gelation stage. Once the gelation is complete, and the level of solvent has dropped below the height of the packed solids, capillaries start to form to facilitate further solvent evaporation. As all the remaining solvent leaves the coating through the capillaries, we get the final solid structure. Deviations to the above outline can arise for each unique drying process, and combinations of materials used.

During the drying process, the coating is susceptible to cracking. Cracks in the electrode for PEMFCs are not necessarily bad. Some controlled cracks have been shown to improve water and mass transport properties [5]. But uncontrolled cracks are bad for durability and can lead to sections in the coating flaking off resulting in poor electrode quality. For these reasons it is desirable to have crack free coatings. Cracks are caused by an interplay of capillary forces, electrostatic and van der Waals forces in the drying layer [5]. Of these forces, the capillary pressure induced compressive forces when solvent vapors push through pores formed while drying are one of the leading factors causing cracks [7].

Studies on the drying process specific to catalyst inks for PEMFCs are limited. However, some indications on various aspects of the process can be gathered from a few sources. Using contrast-variation small-angle neutron scattering (CV-SANS) method, it was seen that both the size of the carbon agglomerates and the thickness of the ionomer shells decrease with increasing ink concentration, which can be attributed to the exclusion of solvent molecules from the carbon and ionomer agglomerates during the drying process [6]. More cracks were observed during drying when the interaction between the ionomer and catalyst particle in the ink was not good [6]. Visualizations of the drying mechanism are often simplified in different studies as solvent leaving only in the direction perpendicular to the plane of the coating. However, it should be noted that a drying front is often observed to move in the in-plane direction of the coating starting from the edges and moving into the bulk of the coating [5]. This suggests that there is mass transfer of solvent leaving the wet coating as it evaporates, in the in-plane direction also. Capillary stress during drying is inversely proportional to pore size (or the capillary diameter). Bigger uniform pores are better for lower stresses and less cracks [7]. Better ionomer and catalyst dispersion promotes the formation of uniform and bigger pores. Combining such studies with a general outline of drying can help build a better picture of the drying process specific to the one studied here.

2.2. Quantitative measures to study cracks

To compare electrode quality in terms of cracks, quantitative measures are important to avoid discrepancies. Cracks density, which is defined as the total length of cracks divided by the sampled area is one such metric [9]. Another metric is the average width of cracks, and this in combination with crack length can be used to estimate the total cracked area [9]. These are interesting parameters to describe cracks quantitatively, but it requires good image processing programs run on several digital microscope images, to estimate these metrics in a systematic way.

Another interesting way to describe the tendency of a coating to crack is Critical Crack Thickness (CCT). CCT is the coating thickness threshold beyond which cracking starts to happen [7]. CCT can be expressed in the equation $h = (2GE/Z\sigma^2)$, where h is CCT, G is fracture toughness, E is Young's modulus, Z is a constant expressing the geometry of the crack tip and σ is the biaxial tensile stress. Coatings made from each ink have a certain characteristic fracture toughness as it dries, and if the drying stresses exceeds this, it cracks. A higher CCT indicates a higher fracture toughness as seen from the equation above. Better crack free coatings can be achieved by well dispersed ionomer and Pt/C in the ink [7]. Coatings with the same ink can be made at increasing thickness to measure its CCT. Depending on the resources available, this method can make for a simple way to rate inks and coatings and their tendency to crack quantitatively.

2.3. Solvent impact on catalyst ink and drying

The solvent medium used to make the catalyst ink is a crucial factor that can strongly influence the ink structure and the drying process. Solvents for PEMFC catalyst inks are typically an alcohol water mixture. When choosing the solvent medium, some common parameters considered are the choice of alcohol, and the water to alcohol ratio. How these parameters can affect the ink structure, and subsequently the drying process is discussed below.

The solvent medium impacts various aspects of the ink structure like the catalyst particle size distribution, the morphology of the ionomer and how the ionomer interacts with the catalyst particles. When 1-propanol (NPA), 2-propanol (IPA), ethylene glycol (EG) and 1,2-butanediol (BUT) were used in a 3:1 alcohol is to water ratio as the solvent medium, it was seen that the solvent choice affected both electrode structure and the performance and durability [10]. It was seen that using IPA led to more cracks in the coatings, because IPA is symmetric and does not enable stabilizing the dispersed catalyst particles by forming solvent miscella around them, like NPA can. While using NPA gave a better initial performance, EG and BUT solvent media resulted in better durability of the electrodes. The solvent affecting the ionomer distribution around the catalyst particles was discussed as the main cause of this. Gel point for ionomer varies for different solvents. A lower gel point can help with more gelling and a good lamellar structure while drying. More polar solvents will have a higher gelation concentration. So less polar solvent medium is more desirable for more gelation while drying [10].

Studies on water alcohol ratio on ink structure and drying are not always in agreement. Some studies [11] suggest that a higher NPA concentration in the ink leads to larger ionomer aggregates. Such aggregated ionomer structures lead to bad quality in resulting electrodes. Water rich inks were seen to have more Pt to sulphonate interaction. No significant difference was observed in just the carbon aggregate size with ink water content. Other reports [12] suggest that higher NPA content is beneficial and that higher water content in inks increases agglomeration. The ionomer was seen to form aggregates or miscella structures in water rich solvents and a more expanded structure in NPA rich solvents by virtue of increased hydrophobic interactions among the methyl group of the alcohol and the fluorocarbon-based ionomer backbone. Similar interactions can also lead to smaller catalyst aggregates in NPA rich solvents. When considering the morphology of the ionomer in the ink, it is interesting to make a distinction between ionomer particles that are adsorbed on the catalyst surface as opposed to ionomer that is free in the solvent. A solvent medium that is less polar leads to the ionomer being removed from the Pt/C and forming free ionomer in the ink [7]. These free ionomers are self-organizing structures that lead to stress concentration and cracks while drying. More ionomer adsorbed on Pt/C can lead to better binding action. With these considerations of solvent impact on the ink in mind, it is important to think about how much a certain ink structure will extend itself to the final dried structure of the coating and how much it will change. Cryo-SEM was used to analyze ink microstructure in relation to dried electrode structures [12]. Similar images in both cases suggested ink structure might extend itself in a comparable way to the dried electrode structures. This could mean solvent choice should consider a desirable ink structure first, and optimizing solvent medium for its impact on the drying process alone would be constrained by this to some extent.

During the drying process, as the solvent evaporates, both the proportion of the alcohol and water in the solvent and the solid to solvent concentration changes constantly. These changes are difficult to measure and previous studies on structural evolution as response to these changes are limited. One study [8] showed that inks or pastes with fast-evaporating solvents (lower aliphatic alcohols like ethanol and NPA evaporate faster than water) are more prone to mud-cracking. This could be due to higher drying stresses at a faster drying rate. This makes drying time an interesting parameter to study. Another important process parameter in drying is the temperature. Previous studies on this topic are also very limited. The lack of understanding and previous studies around many aspects of the drying process adds to the importance of building further competence in this key area of the electrode manufacturing process.

3. Methods

3.1. Process of making PEMFC electrodes

3.1.1. Ink mixing

The electrode making process starts by mixing all three components of the ink (platinum catalyst particles on carbon support, poly fluoro sulphonic acid (PFSA) based ionomer solution and a solvent mixture of alcohol and water). Components are measured by weight to ensure repeatable proportions in the ink.

Figure 3.1: Weighing balance to measure and mix ink components to proportion.

A weighing balance inside a fume hood is used for this purpose as shown in Figure 3.1. The ink is made in a glass or plastic bottle.

3.1.2. Dispersion and maturation

Once the components are mixed, the ink bottle is left in a magnetic stirrer (Figure 3.2) for 1 hour at 300 rpm. The catalyst ink is then dispersed using an ultrasonic dispersion device (Figure 3.2), where a dispersion probe or sonotrode is dipped in the catalyst ink and is excited ultrasonically, creating high pressure air bubbles in the ink and breaking down the particles to a finer mixture. A 7mm diameter sonotrode is used, a total dispersion energy of 50kWs (per 20g of ink) is put into the ink and the excitation amplitude of the probe is set to 50%. A water bath is used to prevent overheating of the ink while dispersing. The ink is then put back into the magnetic stirring station for 1 day and stirred at 300rpm as a maturation

step and to de-gas the ink. Initial experiments in this master thesis have used the dispersion method mentioned above, which will be called dispersion method 1 going forward. And for later experiments an additional roller shaker dispersion step (Figure 3.4) has also been added to the process. It has been described in the results section when this new dispersion process is introduced. This new dispersion process involves the same steps as described above till the ultrasonic dispersion. After this, the final maturation step is replaced with a roller shaker dispersion step. For the roller shaker dispersion step, the ink is dispersed for 2 days, using 4mm diameter Zr beads. The total weight of beads used is two times the ink weight. This additional dispersion step is used after the ultrasonic dispersion step to further grind down the catalyst particles. This dispersion process will be called dispersion method 2 going forward.

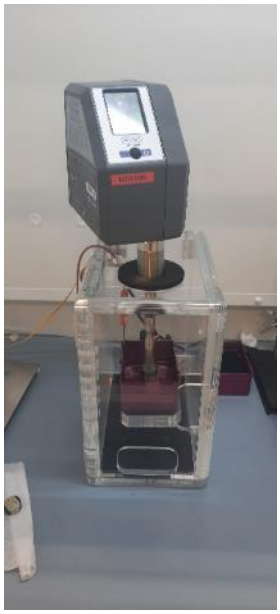

Figure 3.2: Ultrasonic Disperser

Figure 3.3: Magnetic stirring station

Figure 3.4: Roller shaker in use with 5 ink bottles

3.1.3. Coating the ink on the decal substrate

Once dispersed and matured, the catalyst ink is now ready to be coated on to the decal substrate. The decal substrate is a polymer sheet, typically PTFE based. The decal is cut out and set on a linear drive stage with a vacuum base (Figure 3.5). A Doktor blade (Figure 3.5) is then set to a desired coating height and placed on the coating station over the decal. The catalyst ink is pipetted out in front of the Doktor blade, and the linear drive pushes it forward at a set speed to coat the ink on the decal.

Figure 3.5: Doktor blade on the linear drive stage with a vacuum base

3.1.4. Drying the catalyst coating

The coated electrode is now transferred carefully on to a drying box (Figure 3.6) where it is left undisturbed, to dry in a closed environment at room temperature. Drying in this way typically takes 4 hours. Drying is also done for some experiments in a Moisture Analyzer (Figure 3.7) device where higher temperatures and a nitrogen filled environment can be used. Some experiments also have an open bottle of solvent inside the drying box so the effects of a higher vapor pressure above the coating can be studied.

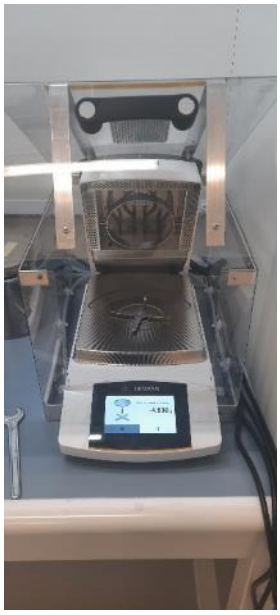

Figure 3.7: Moisture Analyzer device for higher temperature drying in a nitrogen environment.

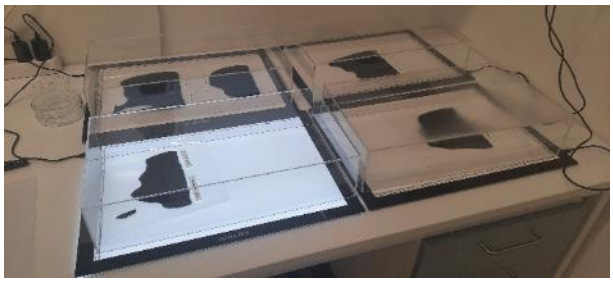

Figure 3.6: Drying box station with a light board base.

3.2. Description of materials used

1. Catalyst A: Platinum on high surface area carbon.

2. Ionomer A: Poly fluoro sulphonic acid (PFSA) based, short side chain, low equivalent weight ionomer material.
3. Solvents: Ethanol, 1-Propanol (NPA), tert-butanol, de-ionized (DI) water.
4. Decal substrate: PTFE based polymer films.

3.3. Characterization

3.3.1. Rheology

Rheology describes the viscoelastic properties of the ink. Viscosity measurements over increasing shear rates and oscillatory measurements of increasing shear amplitude are used for characterization here. Oscillatory measurements performed at 1Hz frequency give the elastic modulus (G') and loss modulus (G'') values for the ink. A small sample of the ink is transferred on the rheometer (Figure 3.8) after the dispersion process, before the ink is coated on the decal.

Figure 3.8: Rheometer

The rheometer has a conical probe to shear the liquid, a solvent box to prevent drying while testing, and a measurement stage with active temperature control where the sample can be poured. Rheology is a powerful tool to understand the interactions in the ink and for defining the optimal properties for the coating process and storage of inks.

3.3.2. Digital microscope

Digital microscope (Figure 3.9) images are taken after the coating dries to study final electrode structures. Lower magnification images are used to get an overview of cracks in the coatings and higher magnification images are used to investigate the presence of bigger

agglomerates and crack morphology. Qualitative analysis of the microscope images of the dried coatings is the main tool used in this study to evaluate electrodes.

Figure 3.9: Digital microscope

3.3.3. Catalyst loading measurements

The dried electrode coatings are cut into pieces of known areas with a blade die and press (Figure 3.10). These cut sections are weighed, and then weighed again after the coating is rubbed off with wet and dry wipes. The weight difference divided by the area multiplied by the fraction of platinum weight to total weight gives the platinum loading of the section. The unit for platinum loading used here is milligram per centimetre squared.

Figure 3.10: Blade, die and manual press.

4. Results and Discussions

4.1. Baseline ink and coatings

Initial experiments were done to set up a baseline electrode making process and changes made to this later were compared to the results here. Baseline ink composition used was as follows: materials used were catalyst A, ionomer A, NPA and water. Solid content of 12.6% (ratio of solid materials to liquid solvent materials), ionomer to platinum ratio (I/C) of 1, 3:2 ratio of NPA to water in the solvent. Dispersion method 1 was used on this ink composition. Coatings were made at a coating height of 100 microns and 150 microns set on the Doktor blade at a coating speed of 50 mm/s and 75mm/s respectively. The ratio of coating height to coating speed was kept constant to maintain similar shear forces on the ink. Decal A is used as the baseline decal material. The coatings were dried under a closed box. Microscope images were taken to assess coating quality. The results are shown in figures 4.1 and 4.2.

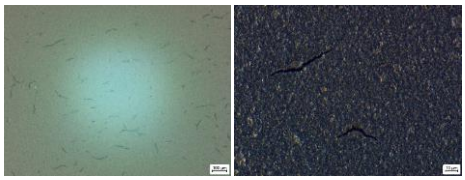

Figure 4.1: Microscope images for 100 microns coating height, low magnification image on left, high magnification image on right.

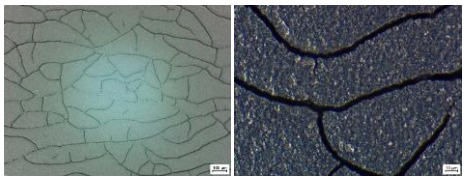

Figure 4.2: Microscope images for 150 microns coating height, low magnification image on left, high magnification image on right

Note that the difference in color seen in most of the higher magnification images is due to a different light setting used for better visibility of particles that stand out of the coating. Microscope images showed that at 100-micron coating height, some isolated cracks were seen, and at 150-microns coating height, much bigger and spread-out cracks were observed. The higher magnification images showed the presence of some agglomerates or particles of around 10 microns, and the cracks seem to have formed around these particles. The critical crack thickness (CCT) for coatings from the baseline process was around 100-microns coating height or less, since cracks were already observed at this height.

4.2. Solid content experiments

The solid content was changed to 10%, 15% and 20% from the baseline process (12.6%) keeping all other parameters constant. Coatings were made at 100-micron coating height. Microscope images were taken to assess coating quality. Results can be seen in Figure 4.3.

Figure 4.3: Microscope images for 10, 15 and 20% solid content ink coatings from left to right respectively

It was seen that all three ink compositions gave worse coating quality crack wise, compared to the baseline process coatings at the same 100-micron coating height. The 10% solid content ink resulted in a higher crack frequency and the 15 and 20% solid content inks gave bigger and more spread-out cracks. The 20% solid content ink also showed bigger undispersed particles in the coatings in a size range of ~50 microns.

These results suggest that for the baseline process, a 12.6% solid content is closer to an optimum than any of the lower or higher solid contents tried. It can also be inferred that for a certain dispersion process, increasing the solid content beyond an optimum value can lead to poorer dispersion results.

4.3. Ionomer to Platinum ratio (I/C) experiments

The I/C ratio was changed by adding more and less ionomer with respect to the catalyst, keeping the amount of catalyst and solvent the same as the baseline. I/C ratio was changed to 0.7 and 1.3 from a value of 1 for the baseline process. The rest of the parameters are kept the same. It must be noted that the dry weight of the higher I/C inks will be slightly higher and vice versa. Coatings were made at 100-micron coating height. Microscope images were taken to assess coating quality. Results can be seen in Figure 4.4 and 4.5.

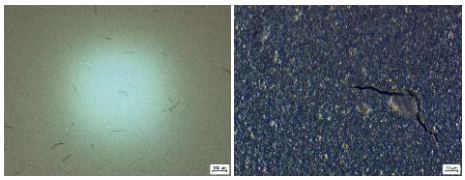

Figure 4.4: Microscope images for I/C 0.7 ink coatings from left to right at low and high magnification respectively.

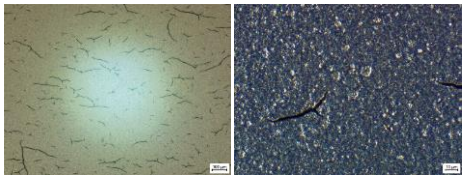

Figure 4.5: Microscope images for I/C 1.3 ink coatings from left to right at low and high magnification respectively.

Results showed that the least cracks were observed for an I/C of 0.7, and most cracks were observed for I/C of 1.3. The higher magnification pictures showed that there were more undispersed particles in the coatings from the I/C 1.3 ink.

One of the main functions of the ionomer in the ink is to act as a binder and hold the coating together, preventing cracks. So, adding more ionomer leading to more cracks is not an expected result. The reason for such a behavior could be due to the presence of more free ionomer groups in this ink that was not adsorbed on to the catalyst, which led to higher stress concentrations as it dried, as discussed in the theory section previously. The bigger agglomerates could have been stabilized by the presence of excess ionomer, which prevented further dispersion of these particles. More such bigger particles will also lead to sites of higher stress concentrations during drying, thus inducing more cracks.

4.4. Solvent experiments

Different alcohols were used at different alcohol to water ratios for the solvent medium in the following experiments. The rest of the parameters were kept the same as for the baseline process. The alcohols used were 1-propanol (NPA), ethanol, and tert-butanol. The solvent to alcohol ratios tried were 20, 40, 60 and 80% alcohol in water. Note that the 60% NPA solvent medium was the baseline process. So, these results were not repeated here. The 80% tert-butanol ink was very thick and difficult to handle, so this combination was also left out of the results. Coatings were made at 100 and 150-micron coating height. Microscope images were taken to assess coating quality. Results are discussed in the following sections. Shorthand notations were used to describe each solvent combination. H denotes water, N denotes NPA, E denotes ethanol, T denotes tert-butanol, and the numbers following the sequence of letters denotes the ration of the respective materials in the

solvent medium. For example, in the shorthand HN23, H is water, N is NPA and the ratio of water to NPA is 2:3.

4.4.1. NPA

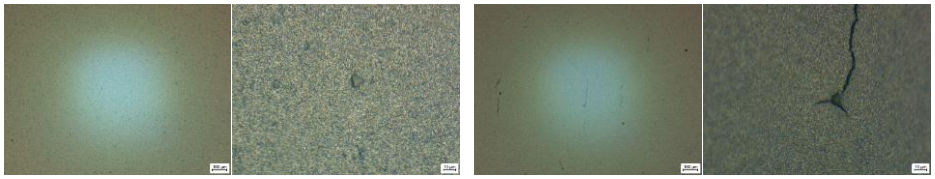

Figure 4.6: Microscope images for HN14 solvent medium inks at 100-micron coating height in low and high magnification, 150-micron coating height in low and high magnification from left to right respectively.

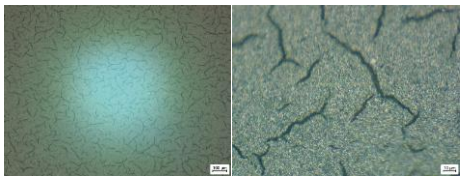

Figure 4.7: Microscope images for HN32 solvent medium inks at 100-micron coating height in low and high magnification from left to right respectively.

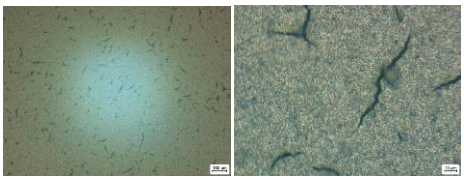

Figure 4.8: Microscope images for HN41 solvent medium inks at 100-micron coating height in low and high magnification from left to right respectively.

The results here showed that the least cracks were observed when 80% NPA was used in the solvent medium. The coatings at 100-micron coating height did not show any cracks, for this ink and the coatings at 150-micron coating height only showed isolated cracks around some undispersed particles in the ink. CCT for this ink would be around 150-micron coating height. Inks with 40% NPA and 20% NPA gave worse results compared to the baseline in terms of cracks. Bigger undispersed particles were observed in the 20% NPA inks in the size range of 10 microns, and cracks were observed to form around these bigger particles.

It can be inferred that inks with higher NPA content (80%) resulted in coatings with a higher fracture toughness and CCT. Supplier data suggests that ionomer A swells in NPA rich media. This could be due to the polymers in the ionomer going from a coiled miscella like structure to a more expanded structure and entangling with each other. Such an ionomer morphology can provide a better binding action in the coatings. This could be the reason behind the improved crack resistance seen here. The water rich inks seem to show a higher tendency of

agglomeration as seen in some previous studies. This could explain the worse results in the 20% NPA inks.

4.4.2. Ethanol

For all the microscope images in the section below, from left to right, coatings are shown at 100-micron coating height in low and high magnification, 150-micron coating height in low and high magnification respectively.

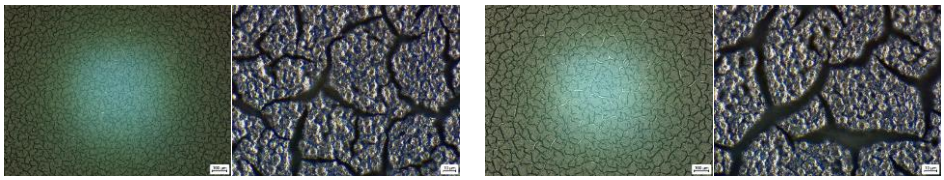

Figure 4.9: HE14

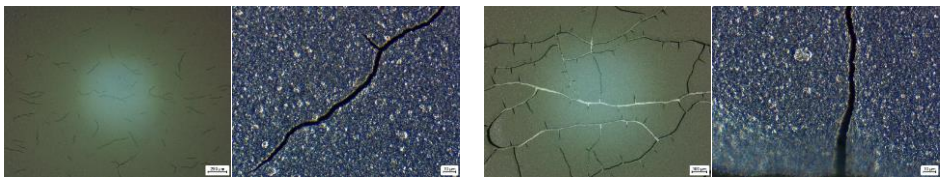

Figure 4.10: HE23

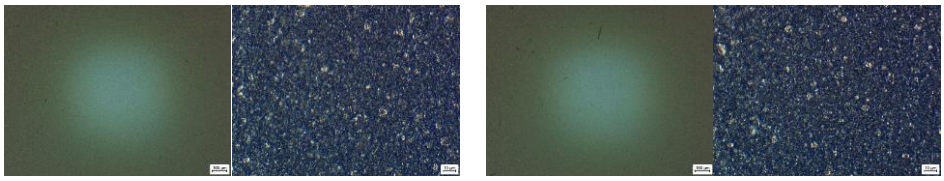

Figure 4.11: HE32

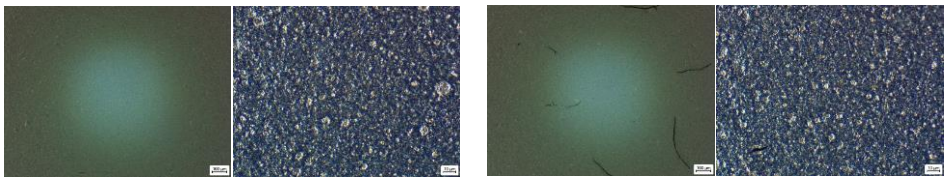

Figure 4.12: HE41

When ethanol was used as the alcohol in the solvent, the worst coating quality was observed for the highest ethanol content inks (80% ethanol) in terms of cracks. The coatings here also show very high presence of agglomerates in the ink at a size range of 5 microns. Coating quality progressively improved with increasing water content and showed an optimum at the 60% water 40% ethanol composition. The CCT can be seen to improve to around 150-micron coating height in this case. Results worsened slightly for the 80% water 20% solvent composition, as can be seen when comparing the 150-micron coating images.

These results are difficult to explain and need further evaluation. Previous studies on the impact of changing ethanol content in catalyst inks are limited.

4.4.3. Tert-butanol

For all the microscope images in the section below, from left to right, coatings are shown at 100-micron coating height in low and high magnification respectively.

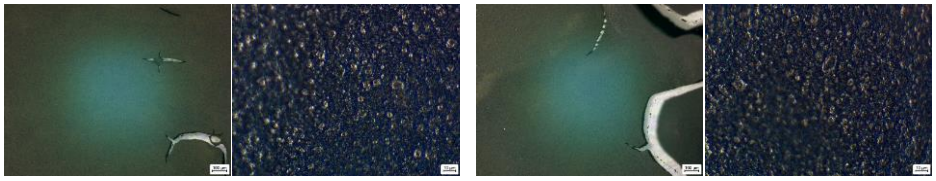

Figure 4.13: HT23

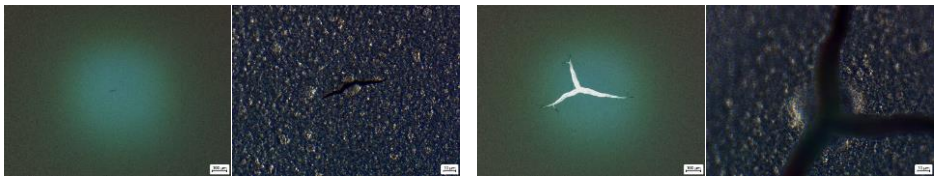

Figure 4.14: HT32

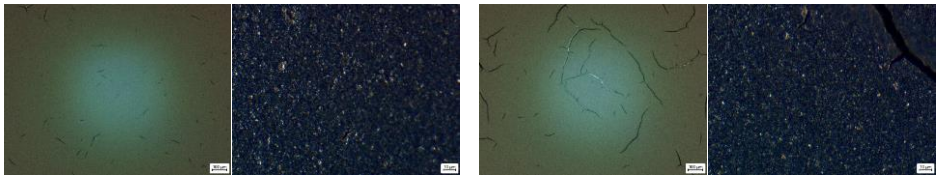

Figure 4.15: HT41

Higher tert-butanol content (80% and 60%) in the inks resulted in very thick dispersion that are not easy to handle from a processing point of view. The results here follow the same trend as in the case of NPA in section 4.4.1, except that at higher tert-butanol contents, the ink became too thick to practically work with.

4.5. Decal experiments

Note that for the all the remaining experiments, dispersion process 2 is used. This involves an additional dispersion step with the roller shaker after the ultrasonication step. For the decal experiments, the baseline ink was coated on 4 different decal materials A, B, C and D. For all the microscope images in the section below, from left to right, coatings are shown at 100-micron coating height in low and high magnification, 150-micron coating height in low and high magnification respectively.

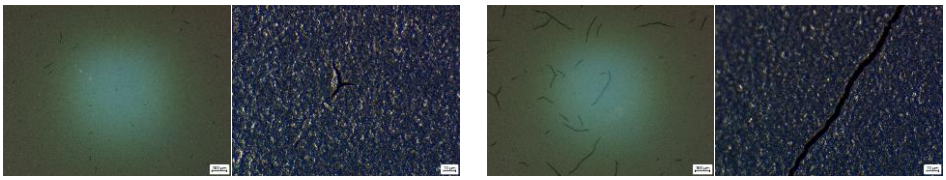

Figure 4.16: Decal A

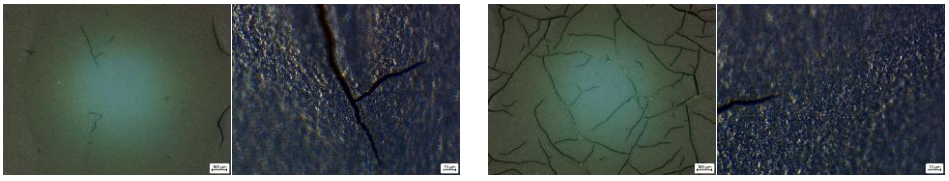

Figure 4.17: Decal B

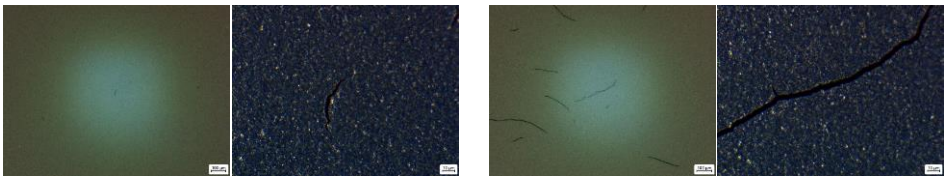

Figure 4.18: Decal C

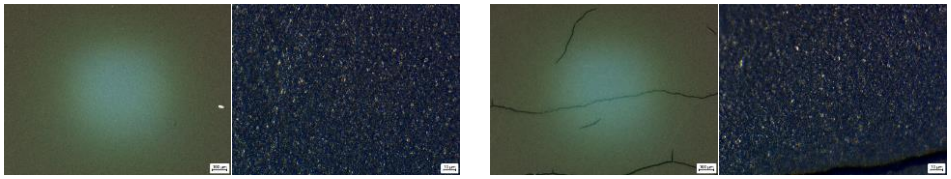

Figure 4.19: Decal D

The results for the decal experiment did not show any significant impact to CCT. The crack morphology was different between the different decals. The most obvious observation here is the coatings on Decal B. Decal B has patterns on its surface due to reinforcements present in it. The cracks on decal B also followed a similar pattern suggesting this non-uniformity of the decal surface roughness added more drying stress leading to cracks.

4.6. Contact angle measurements for Decal

Sample	γ_s^d	γ_s^p	γ_s
Decal A	16.7	3.2	19.9
Decal B	9.9	1.3	11.2
Decal C	37.3	0.3	37.6
Decal D	7.0	0.0	7.0

Table 4.1: Calculated surface energies (in mN/m) for respective sample. γ_S^d is the nonpolar contribution, γ_S^p the polar contribution and γ_S the total surface energy.

This investigation was done externally to obtain surface energy data for the 4 decal material samples. Contact angle measurements are a common technique to determine surface properties of different materials. The results showed that all 4 decal materials have quite different surface properties. However, since no significant difference was seen in the microscope pictures of the coatings between decal A, C and D, it can be concluded that the surface properties of the decal do not have a strong influence on the cracking behavior of the coatings.

4.7. Drying experiments

4.7.1. Higher temperature drying of baseline inks

Coating height (microns)	Temperature (°C)	Drying time (s)	Evaporated solvent weight (g)	Drying time/Evaporated solvent weight (s/g)
100	40	174	0.029	6000.0
	60	138	0.049	2816.3
	80	126	0.074	1702.7
125	40	234	0.070	3342.9
	60	162	0.071	2281.7
	80	120	0.082	1463.4
150	40	300	0.087	3448.3
	60	156	0.092	1695.7
	80	132	0.098	1346.9
	100	126	0.107	1177.6

Table 4.2: Normalized drying times for higher temperature drying of baseline inks.

Table 4.2 shows the different experiments done at higher temperatures for the baseline process. The end of drying was measured using the moisture analyzer device, from its standard control program, when weight change of the wet coating becomes lower than a preset value for a preset amount of time. The drying time was calculated this way from the device, and this is displayed here. Normalized drying time was also evaluated to compare between the samples since the coatings at higher coating heights will have a higher total weight of ink in them. It was seen that the drying is faster at higher temperatures, which is expected. The normalized drying time was seen to increase for the thicker coatings at the same temperatures. This could be due to the initial evaporation rate being higher than the final evaporation rate, and the effect of this showed in a more pronounced way when there was a higher initial weight of ink. It was also seen that for similar coatings, as the temperature was increased, the total weight of vaporized solvent also increased. This could suggest that there was some remaining solvent even after drying was measured as completed by the moisture analyzer, and that a higher temperature was necessary to

completely remove all solvent from the coating. Microscope images for the experiments in Table 4.2 is shown below.

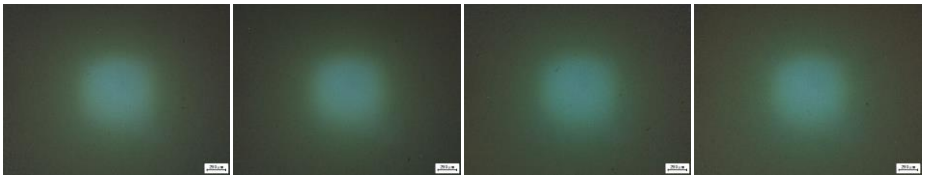

Figure 4.20: Microscope images for coatings at 100-micron coating height, left to right – dried at room temperature, 40 °C, 60 °C and 80 °C respectively.

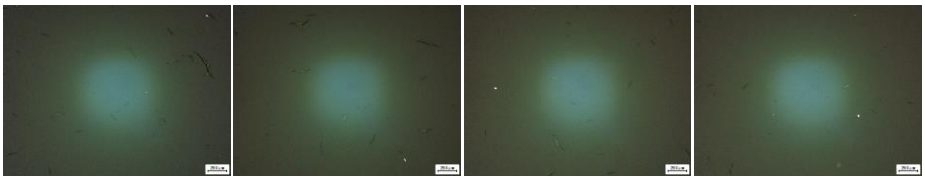

Figure 4.21: Microscope images for coatings at 125-micron coating height, left to right – dried at room temperature, 40 °C, 60 °C and 80 °C respectively.

Figure 4.22: Microscope images for coatings at 150-micron coating height, left to right – dried at room temperature, 40 °C, 60 °C, 80 °C and 100 °C respectively.

For the coatings at 100-micron coating height, no significant difference was observed in the coatings as drying temperature was increased as seen in Figure 4.20. At 125-micron coating height, a slight decrease in crack length was observed with increasing drying temperature as seen in Figure 4.21. At 150-micron coating height, it was seen that at room temperature very long and wide cracks were observed after drying. And as the drying temperature was increased, the width and length of these cracks decreased. It was also seen that the frequency of cracks may have gone up as the drying temperature was increased for these coatings.

To summarize, the higher temperature did not cause more cracks in any of the cases studied. And at higher coating heights, the higher drying temperature seems to have prevented a widening of cracks which was observed when dried at room temperature.

4.7.2. Higher vapor pressure drying of baseline inks

In the higher vapor pressure experiments, an open solvent bottle was used inside the drying box to increase the vapor pressure of the alcohol (NPA here) above the coating. The rest of the parameters of the process were kept the same as the baseline process. Coatings were made at 100 and 150-micron coating height. The drying takes much longer to complete in this case and the coatings were left overnight inside the box. Microscope images were taken of the dried coatings. Results are shown below.

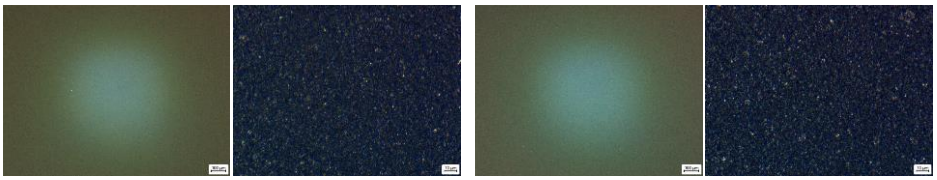

Figure 4.23: Microscope images for coatings at 100-micron coating height at low and high magnification, and at 150-micron coating height at low and high magnification from left to right respectively, dried at higher vapor pressure

This drying method was seen to improve the cracks observed in the coatings significantly. The coatings remained crack free at 150-micron coating height and CCT in this case would be even higher. The higher vapor pressure of the NPA above the coating is expected to slow down the evaporation of the NPA in the wet coating. This may have left the coatings NPA rich for longer as it dried, compared to the previous drying method. This could be a reason behind the results seen here.

4.8. Higher catalyst loading experiments

From the previous experiments, a down selection was made for the ink with the solvent composition of 80% NPA in the solvent medium since it showed a higher fracture toughness and CCT. Dispersion process 2 was used on this ink composition. This ink was used to make coatings at increasing coating heights of 150, 200 and 250 microns and the catalyst loading for these coatings were measured. Four squares of 9cm2 area were cut out of the dried coatings and an average catalyst loading and standard deviation for the loading were estimated. Microscope images were taken for the coatings at 250-micron coating height. Results are summarized below.

Coating height (microns)	Average catalyst loading (mg/cm^2)	Standard deviation (mg/cm^2)	Standard deviation/Average catalyst loading
150	0.436	0.012	2.8%
200	0.565	0.014	2.5%
250	0.712	0.015	2.1%

Table 4.3: Catalyst loading measured for each gap height

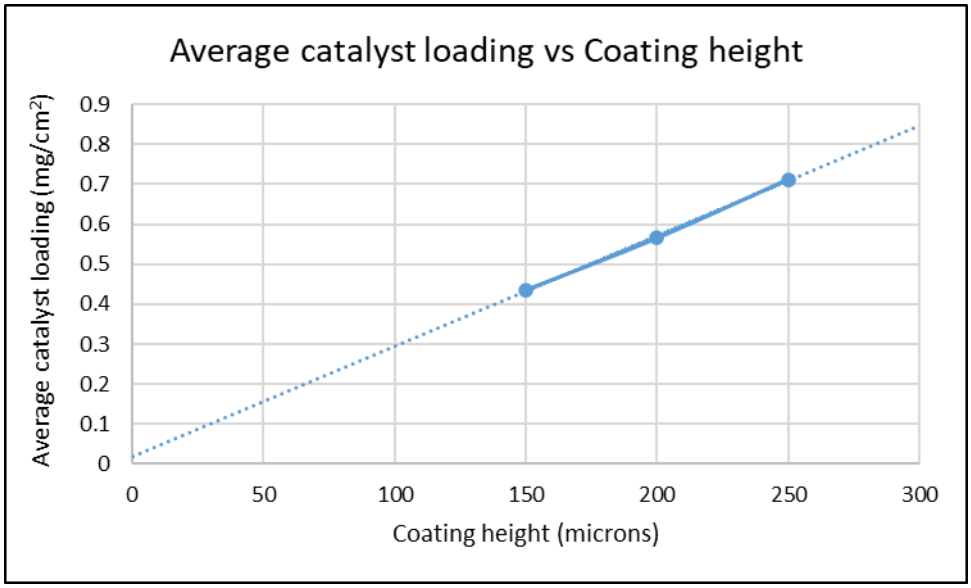

Figure 4.24: Graph of catalyst loading vs coating height showing a linear trend.

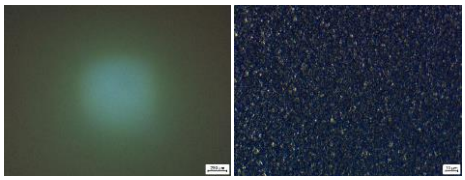

Figure 4.25: Microscope image for coatings at 250-micron coating height with an HN14 solvent composition, from left to right at low and high magnification respectively.

A linear trend was observed when the average measured catalyst loading was plotted against the coating height. The coatings did not show any cracks at a 250-micron coating height, where an average catalyst loading of 0.712 mg/cm2 was measured at a standard deviation of 0.015 mg/cm2.

5. Conclusion

The impact of key drying parameters on PEMFC electrodes was assessed and used to improve quality and processing capability in this master thesis. It was shown that achieving a desirable catalyst ink structure was a crucial first step to get good results after the drying process for electrode coatings. Among the drying parameters studied here, the drying temperature was shown to not impact coating quality adversely. This permits the use of higher temperatures to dry coatings faster after the current ink process and improve throughput without compromising quality. A higher vapour pressure of the alcoholic solvent above the coating while drying was shown to improve the electrode quality, adding insights to the understanding of the drying process.

The studies here have also helped in identifying areas that are interesting for future investigation around this topic. The results here demonstrate the importance of addressing more aspects of the overall drying environment. The impact of higher humidity and the flow rate of solvent vapours above the coating needs to be better understood. Alternative drying methods like infrared drying needs further investigation. The robustness of the impact of drying parameters seen here should be verified for more ink compositions that are relevant for the future. Cracks formation during drying and the forces involved that affect this should be understood to a greater extent theoretically. Further development in any of these topics can add a lot of value to improving the drying process.

Drying is the last step in a multi-step process of catalyst electrode manufacturing. While this makes improvements to this process challenging, it also yields results that directly impact the final electrode structure as seen here highlighting its importance. The improvements already seen at these initial stages of development paints an exciting picture for future work that holds great promise for the transition to green energy.

6. References

[1] “Hydrogen Fuel Cells”, PowerCell Group website, https://powercellgroup.com/hydrogen-fuel-cell/ (accessed April 2023)

[2] Yuqing Guo, Fengwen Pan, Wenmiao Chen, Zhiqiang Ding, Daijun Yang, Bing Li, Pingwen Ming & Cunman Zhang, “The Controllable Design of Catalyst Inks to Enhance PEMFC Performance: A Review”, Nov. 2020, doi: https://doi.org/10.1007/s41918-020-00083-2

[3] Mohammad Ali Abdelkareem, Khaled Elsaid, Tabbi Wilberforce, Mohammed Kamil, Enas Taha Sayed, A. Olabi, “Environmental aspects of fuel cells: A review”, Jan. 2021, doi: https://doi.org/10.1016/j.scitotenv.2020.141803

[4] Meng Xie, Tiankuo Chu, Tiantian Wang, Kechuang Wan, Daijun Yang, Bing Li, Pingwen Ming and Cunman Zhang, “Preparation, Performance and Challenges of Catalyst Layer for Proton Exchange Membrane Fuel Cell”, Oct. 2021, doi: https://doi.org/10.3390/membranes11110879

[5] Lucas Goehring, William J. Clegg, and Alexander F. Routh, “Solidification and Ordering during Directional Drying of a Colloidal Dispersion”, Mar. 2010, doi: https://pubs.acs.org/doi/pdf/10.1021/la100125v

[6] Takumi Kusano, Takashi Hiroi, Kazuki Amemiya, Masaki Ando, Tsuyoshi Takahashi and Mitsuhiro Shibayama, “Structural evolution of a catalyst ink for fuel cells during the drying process investigated by CV-SANS”, Apr. 2015, doi: https://doi.org/10.1038/pj.2015.36

[7] Naomi Kumano, Kenji Kudo, Akihiko Suda, Yusuke Akimoto, Masahiko Ishii, Hiroshi Nakamura Toyota Central R&D Labs., Inc., Nagakute, Aichi, 480-1192, Japan, “Controlling cracking formation in fuel cell catalyst layers”, Apr. 2019, doi: https://doi.org/10.1016/j.jpowsour.2019.02.058

[8] Wentao Wang, Shunquan Chen, Jianjun Li, Wei Wang, “Fabrication of catalyst coated membrane with screen printing method in a proton exchange membrane fuel cell”, Apr. 2015, doi: http://dx.doi.org/10.1016/j.ijhydene.2015.02.027

[9] Florian Mack, Merle Klages, Joachim Scholta, Ludwig Jörissen, Tobias Morawietz, Renate Hiesgen, Dominik Kramer, Roswitha Zeis, “Morphology studies on high-temperature polymer electrolyte membrane fuel cell electrodes”, Jun. 2014, doi: http://dx.doi.org/10.1016/j.jpowsour.2014.01.032

[10] Chao Lei, Fan Yang, Natalia Macauley, Magali Spinetta, Gerie Purdy, Jasna Jankovic, David A. Cullen, Karren L. More, Yu Seung Kim and Hui Xu, “Impact of Catalyst Ink Dispersing Solvent on PEM Fuel Cell Performance and Durability”, Apr. 2021, doi: https://iopscience.iop.org/article/10.1149/1945-7111/abf2b0

[11] Tim Van Cleve, Sunilkumar Khandavalli, Anamika Chowdhury, Samantha Medina, Svitlana Pylypenko, Min Wang, Karren L. More, Nancy Kariuki, Deborah J. Myers, Adam Z. Weber, Scott A. Mauger, Michael Ulsh, and K. C. Neyerlin, “Dictating Pt-Based Electrocatalyst Performance in Polymer

Electrolyte Fuel Cells, from Formulation to Application", Nov. 2019, doi: http://dx.doi.org/10.1021/acsami.9b17614

[12] Shinichi Takahashi, Tetsuya Mashio, Norifumi Horibe, Ken Akizuki, and Atsushi Ohma, "Analysis of the Microstructure Formation Process and Its Influence on the Performance of Polymer Electrolyte Fuel-Cell Catalyst Layers", Jul. 2015, doi: https://doi.org/10.1002/celc.201500131

CHALMERS
UNIVERSITY OF TECHNOLOGY